Molecular dual-rotators with large consecutive emission chromism for visualized and high pressure sensing

Kangming Tan,[a, b] Yan Zeng,[a, c] Lei Su,[a] Shuangqing Wang,[a] Xudong Guo,[a] Qingxu Li,[c] Linghai Xie,[b] Yan Qian,[b] Yuanping Yi,*[a] Wei Huang,[b] and Guoqiang Yang*[a]*

[a]Key laboratory of Photochemistry and Key Laboratory of Organic Solids, Institute of Chemistry, University of Chinese Academy of Sciences, Chinese Academy of Sciences, Beijing 100190, China

[b]Key Laboratory for Organic Electronics and Information Displays & Institute of Advanced Materials (IAM), Jiangsu National Synergetic Innovation Center for Advanced Materials (SICAM), Nanjing University of Posts & Telecommunications (NUPT), 9 Wenyuan Road, Nanjing 210023, China

[c]School of Science, Chongqing University of Posts and Telecommunications, Chongqing, 400065, China

AUTHOR INFORMATION

Corresponding Author

E-mail: iamyqian@njupt.edu.cn, ypyi@iccas.ac.cn, gqyang@iccas.ac.cn

1. Emission spectra and photographs during the pressure-decompressed process

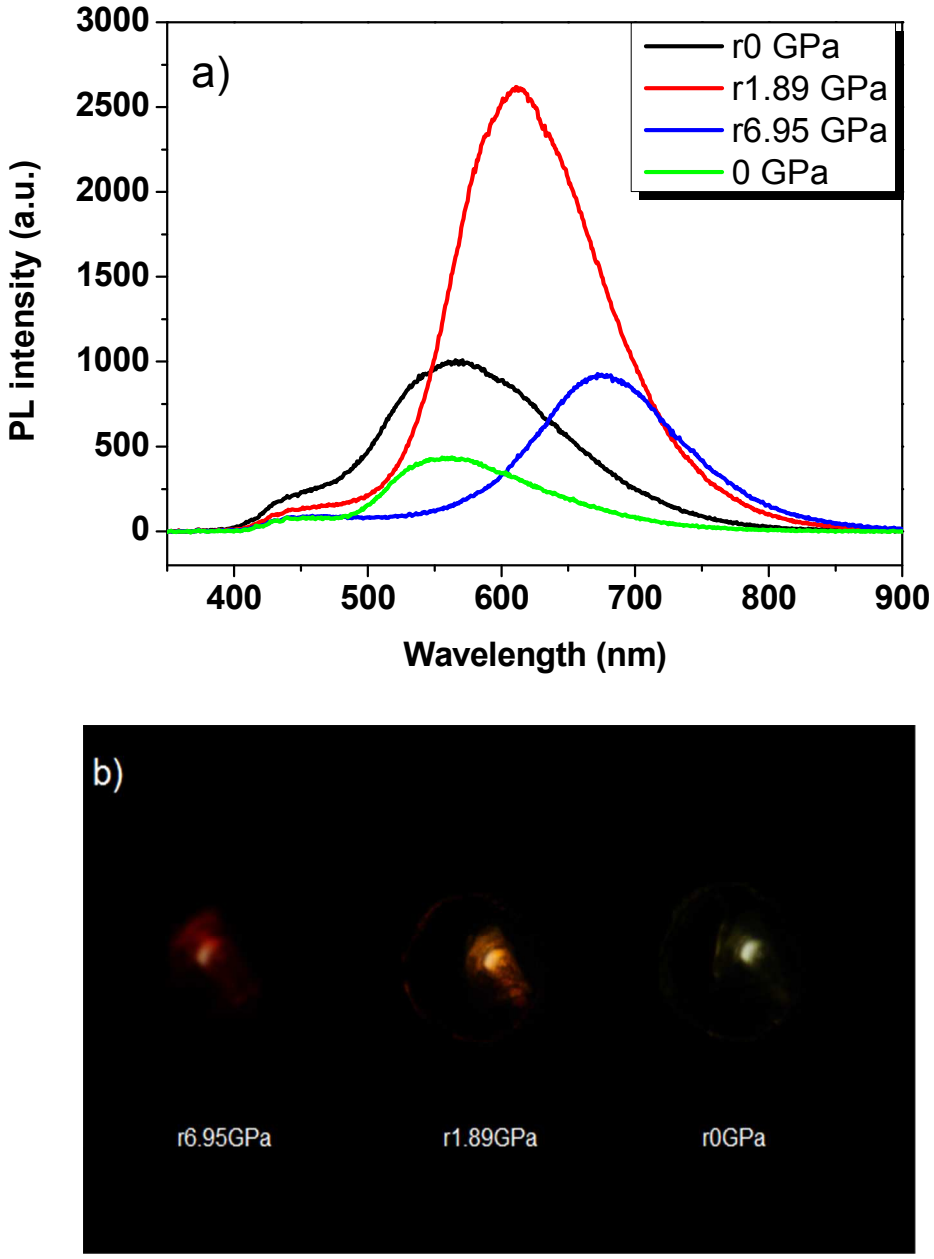

Figure S1. (a) Pressure-dependent fluorescence spectra and (b) Photographic images of DAAD film (0.5 wt% dispersed in PMMA matrix) under different pressures during the pressure-decompressed process (The images were obtained by Canon EOS 5D Mark II). The emission maximums at r6.95, r1.80 and r0 GPa were 675, 612 and 566 nm, respectively.

2. Pressure-dependent fluorescence spectra of DAAD dispersed in PS matrix

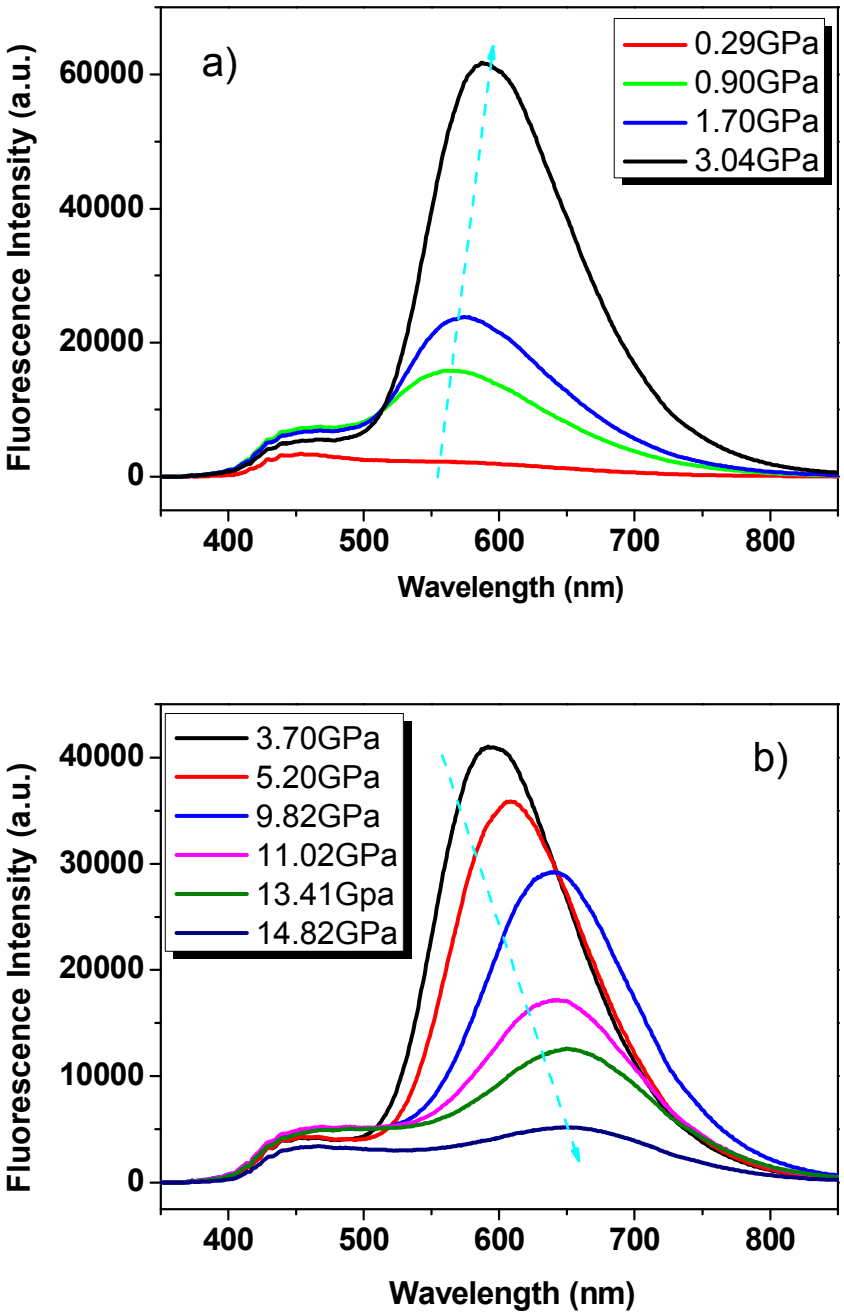

Figure S2. Pressure-dependent fluorescence spectra of DAAD film (0.5 wt% dispersed in PS matrix): (a) emission increasing process; (b) emission decreasing process. The emission peaked around 450 nm is caused by the intrinsic emission from the diamond.

3. Pressure-dependent PXRD patterns of DAAD powder

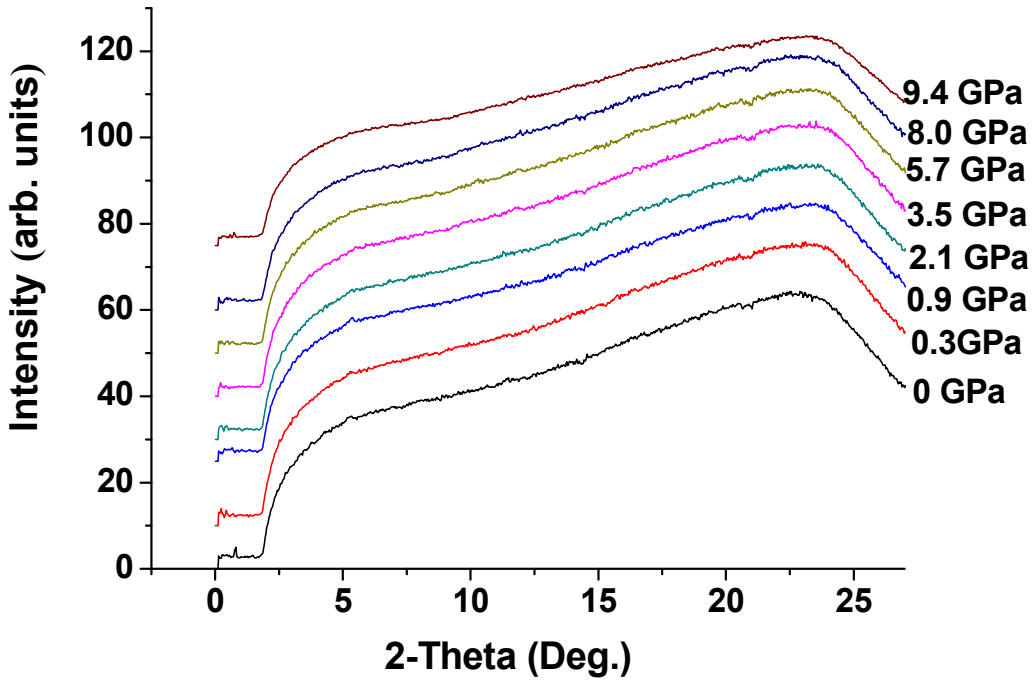

Figure S3. Pressure-dependent PXRD patterns of DAAD powder.

4. Evolution of the S_1 and T_1 excitation energies at the optimized S_1 state as a function of θ_2

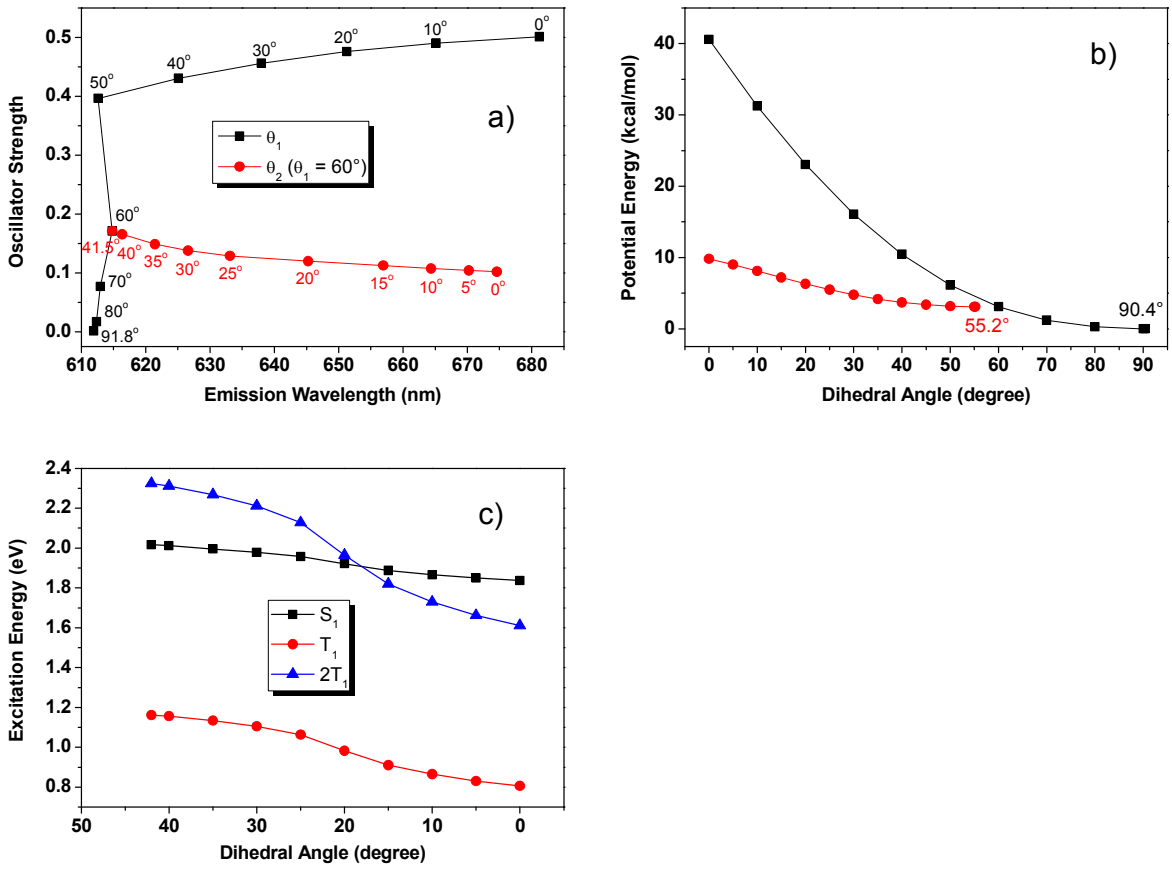

Figure S3. a) Vertical emission wavelengths and oscillator strengths of the S_1 state optimized at different dihedral angles of θ_1 and θ_2 (black: only θ_1 is fixed at different angles; blue: θ_2 decreases from the optimal angle of 48.1° to 0° with θ_1 kept at 50°; c) Relative potential energies of the ground state optimized at different dihedral angles of θ_1 and θ_2 (black: only θ_1 is fixed at different angles; red: θ_2 decrease from the optimal angle of 55.2° to 0° with θ_1 kept at 60°). b) Evolution of the S_1 and T_1 excitation energies at the optimized S_1 state as a function of the dihedral angle θ_2 when the dihedral angle θ_1 is fixed at 50°); c) Evolution of the S_1 and T_1 excitation energies at the optimized S_1 state as a function of the dihedral angle θ_2 when the dihedral angle θ_1 is fixed at 60°, respectively.